doi:10.1016/j.jmb.2003.12.068 J. Mol. Biol. (2004) 336, 1283–1291

JMB

Available online at www.sciencedirect.com

SCIENCE DIRECT®

ELSEVIER

Allosteric Inhibition Through Core Disruption

James R. Horn[1] and Brian K. Shoichet[2]*

[1]*Drug Discovery Program Department of Molecular Pharmacology and Biological Chemistry, Northwestern University School of Medicine 303 East Chicago Ave, Chicago IL 60611-3008, USA*

[2]*Department of Pharmaceutical Chemistry, University of California San Francisco Genentech Hall, 600, 16th Street, Mail Box 2240, San Francisco, CA 94143, USA*

**Corresponding author*

Although inhibitors typically bind pre-formed sites on proteins, it is theoretically possible to inhibit by disrupting the folded structure of a protein or, in the limit, to bind preferentially to the unfolded state. Equilibria defining how such molecules act are well understood, but structural models for such binding are unknown. Two novel inhibitors of β-lactamase were found to destabilize the enzyme at high temperatures, but at lower temperatures showed no preference for destabilized mutant enzymes *versus* stabilized mutants. X-ray crystal structures showed that both inhibitors bound to a cryptic site in β-lactamase, which the inhibitors themselves created by forcing apart helixes 11 and 12. This opened up a portion of the hydrophobic core of the protein, into which these two inhibitors bind. Although this binding site is 16 Å from the center of the active site, the conformational changes were transmitted through a sequence of linked motions to a key catalytic residue, Arg244, which in the complex adopts conformations very different from those in catalytically competent enzyme conformations. These structures offer a detailed view of what has heretofore been a theoretical construct, and suggest the possibility for further design against this novel site.

Keywords: β-lactamase; drug design; cryptic site; core disruption; crystallography

Introduction

Inhibitors typically bind to pre-formed binding sites on proteins, with the resulting complementarity defining our understanding of biological molecular recognition. It has long been known that other sorts of inhibition are possible.[1] Inhibitors can act at sites that are not present in the low-energy "native" conformation of a protein but are accessible through protein conformational change.[2,3] An example is the allosteric inhibition of HIV-RT by nevaripine and analogs.[4,5] Relatively small conformational changes can reveal such sites and correspondingly can disrupt recognition in the substrate site. These revealed sites resemble pre-formed sites, the major difference being their lower equilibrium population. Recent theoretical studies have also suggested more unusual mechanisms. A molecule that binds so as to disrupt the packing or overall structure of a protein, essentially making its own site, will act as an inhibitor if this disruption affects recognition in the active site. In the limit, a molecule that binds preferentially to the denatured state of a protein will act as an inhibitor, even though its affinity for any pre-formed site on that protein might be negligible.[1,6] Mixtures of these extremes are also possible, with interesting consequences for apparent inhibition and stability patterns as recently discussed by Waldron & Murphy (Figure 1).[6] Whereas the linkage equilibria explaining such non-classical inhibitors are well understood, a detailed picture for how they might act has been lacking, owing to difficulties in determining their complexed structures or, indeed, discovering them in the first place.

In an effort to discover novel inhibitors of the antibiotic resistance enzyme β-lactamase, we happened upon two compounds that had unusual properties as enzyme inhibitors. These molecules were non-competitive but also reversible inhibitors. They appeared to bind in a one-to-one stoichiometry with the enzyme, and did not act as promiscuous, aggregation-based inhibitors.[7] At high temperatures they destabilized the enzyme, but at room temperatures they showed no preference for stabilized or destabilized mutant enzymes. They inhibited β-lactamase with some specificity *versus* several unrelated enzymes. Perplexed, we sought to understand their mechanism by determining

Abbreviations used: MDH, malate dehydrogenase; rmsd, root-mean-square deviation.

E-mail address of the corresponding author: shoichet@cgl.ucsf.edu

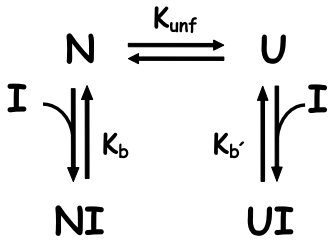

Figure 1. Simplified thermodynamic model for an inhibitor (**I**) that binds both native (N) and unfolded (U) states. A more complete model, with consequences for patterns of inhibition and stability, is given by Waldron & Murphy.[6]

their enzyme-bound structures. Crystal structures of both compounds in complex with β-lactamase were determined to 1.90 Å and 1.45 Å resolution. Unexpectedly, both inhibitors insert themselves between two α-helices 16 Å from the active site, disrupting intramolecular interactions in part of the hydrophobic core of the protein to reveal a cryptic binding site. In binding, these molecules disrupt the core and, through a series of linked conformational changes, alter the conformation of a key catalytic residue. These structures offer a detailed view for a mechanism of inhibition, disruption of the folded conformation, that heretofore has been a construct of equilibria arguments. The prospects for future inhibitor discovery will be considered.

Results

Enzyme inhibition

While pursuing novel inhibitor discovery of TEM-1 β-lactamase, two non-substrate-like molecules were discovered. Inhibition assays demonstrated that both 3-(4-phenylamino-phenylamino)-2-(1H-tetrazol-5-yl)-acrylonitrile (compound **1**) and *N*,*N*-bis(4-chlorobenzyl)-1H-1,2,3,4-tetraazol-5-amine (compound **2**) inhibited TEM-1 non-competitively, with K_i values just under 500 μM (Table 1).

To rule out the possibility that inhibition was the result of promiscuous, non-specific aggregation,[7] several tests were performed. Consistent with specific inhibition, no difference in inhibition was observed when assays were run in the presence or absence of detergents such as Triton X-100 or saponin, which are known to disrupt aggregates.[8] In addition, the compounds did not display an incubation effect when pre-equilibrated with enzyme prior to reaction initiation.[7] Finally, neither compound detectably inhibited two disparate enzymes, malate dehydrogenase (MDH) and trypsin (Table 1),[8] at up to 1 mM concentration. These results rule out aggregation-based inhibition and suggest some specificity for TEM-1 β-lactamase.

Thermal denaturation experiments were performed to further explore the interaction of the compounds with TEM-1. If a compound binds preferentially to a protein's native state, that state will be stabilized relative to the denatured

Table 1. Kinetic characterization and specificity assays of TEM-1 inhibitors

Compound	Structure	K_i (μM) TEM-1	K_i (μM) MDH	K_i (μM) trypsin
1	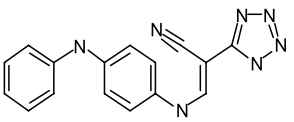	490 ± 40	>4000[a]	>4000[a]
2	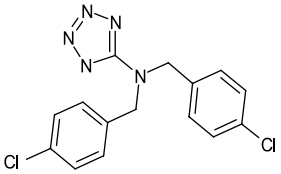	480 ± 20	>4000[a]	>4000[a]
3[b]	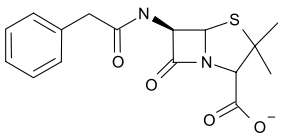			
4[c]	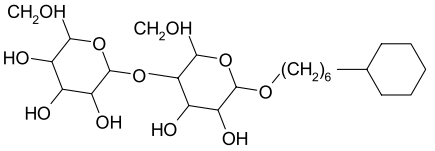			

Measurements made at 25 °C. See Materials and Methods for assay solution conditions.
[a] Inhibition not detected. Tested up to 1 mM compound; minimum K_i predicted assuming 20% inhibition at 1 mM.
[b] Structure of Penicillin G. Drawn to show the dissimilarity of the new inhibitors to classical substrates of TEM-1.
[c] Structure of cyclohexyl-hexyl-β-D-maltoside (Cymal-6) from Knox and co-workers.[18]

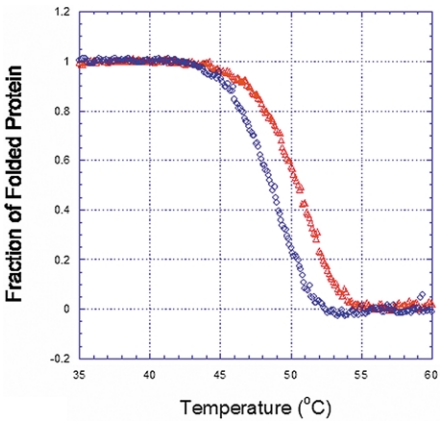

Figure 2. The affect of inhibitor binding on the thermal stability of TEM-1. Apo TEM-1 (red triangles) and TEM-1 with 250 μM compound **2** (blue circles).

Table 2. Melting temperature (t_m) values for thermal unfolding of TEM-1

Wild-type	wt-TEM Compound **1** (250 μM)	wt-TEM Compound **2** (250 μM)	M182T TEM[a]	G238A TEM[a]
51.0	50.1	48.6	57.7	47.0

Conditions for all experiments were performed with 50 mM phosphate buffer (pH 7.0).
[a] The mutant TEM-1 unfolding data have been described.[9]

state and the stability of the protein will increase. Conversely, if a compound binds preferentially to the denatured state, the denatured state will be favored and the stability of the protein will decrease. Intriguingly, in reversible, two-state thermal denaturation studies the presence of either compound resulted in a lower temperature of melting (t_m) for the protein (Figure 2; Table 2). This suggested that both compounds bind preferentially to the denatured state of the enzyme over the native state, at least at high temperatures.

Additional enzyme assays were performed to address the mechanism of inhibition at 25 °C. Two stability mutants of TEM-1 were investigated, an increased stability mutant (M182T) and a decreased stability mutant (G238A).[9] If inhibition worked exclusively through binding to the denatured state, then either inhibitor should have a higher affinity for the destabilized mutant then for the stabilized mutant. However, affinities for the stabilized M182T were comparable to those for wild-type, whereas affinity for the destabilized G238A were actually less than for the WT enzyme (Table 3). This result is inconsistent with binding exclusively to the denatured state, at least at room temperature. The mechanism of inhibition was also investigated by varying the temperature at which inhibition assays were performed. Affinity was greatest at low temperature and decreased with increasing temperature (Table 3). These results suggested that the dominant mode of inhibition at 25 °C differs from that at higher temperature (e.g. during thermal melt experiments). At lower temperatures, inhibition is dominated by binding to some form of the native state, whereas at higher temperatures it is dominated by binding to the unfolded state.

Table 4. Crystal data and refinement statistics for TEM-1 inhibitor complexes

Compound	Compound **1**	Compound **2**
Space group	$P2_12_12_1$	$P2_12_12_1$
Unit cell dimensions (Å)	$a = 41.55$; $b = 60.67$; $c = 89.09$	$a = 41.89$; $b = 61.04$; $c = 88.68$
Resolution (Å) (last shell)	20.0–1.47 (1.58–1.47)	20.0–1.90 (2.09–1.90)
No. of unique refl.	38,464	17,299
Data compl. (%) (last shell)	99.51 (99.8)	98.47 (99.7)
R_{merge} (%) (last shell)	6.0 (44.4)	7.9 (40.8)
No. protein atoms	2030	2026
No. inhibitor atoms	46	44
No. solvent molecules	227	180
Avg. *B*-factor (Å^2; protein)	20.2	17.5
Avg. *B*-factor (Å^2; inhibitor)	32.0	21.9
Avg. *B*-factor (Å^2; water molecules)	31.1	26.8
R_{cryst}/R_{free} (%)[a]	19.3/23.4	19.1/24.7
rms bonds (Å)	0.019	0.023
rms angles (deg.)	1.89	1.94

[a] R_{free} was calculated with 5% of reflections set aside randomly.

Structure

These unusual characteristics motivated crystallographic studies to determine the mode of binding. The structures of TEM-1 in complex with compounds **1** and **2** were determined by X-ray crystallography to 1.45 Å and 1.90 Å resolution, respectively (Table 4). The electron density for both compounds was unambiguous (Figure 3).

Table 3. K_i values for inhibition of stability mutants and temperature studies

Compound	Wild-type (25 °C)	M182T TEM (25 °C)	G238A TEM (25 °C)	Wild-type (15 °C)	Wild-type (36 °C)
1	490 ± 40	480 ± 30	590 ± 20	329 ± 9	810 ± 40
2	480 ± 20	460 ± 10	590 ± 20	370 ± 20	550 ± 20

Values are given in concentration units of μM.

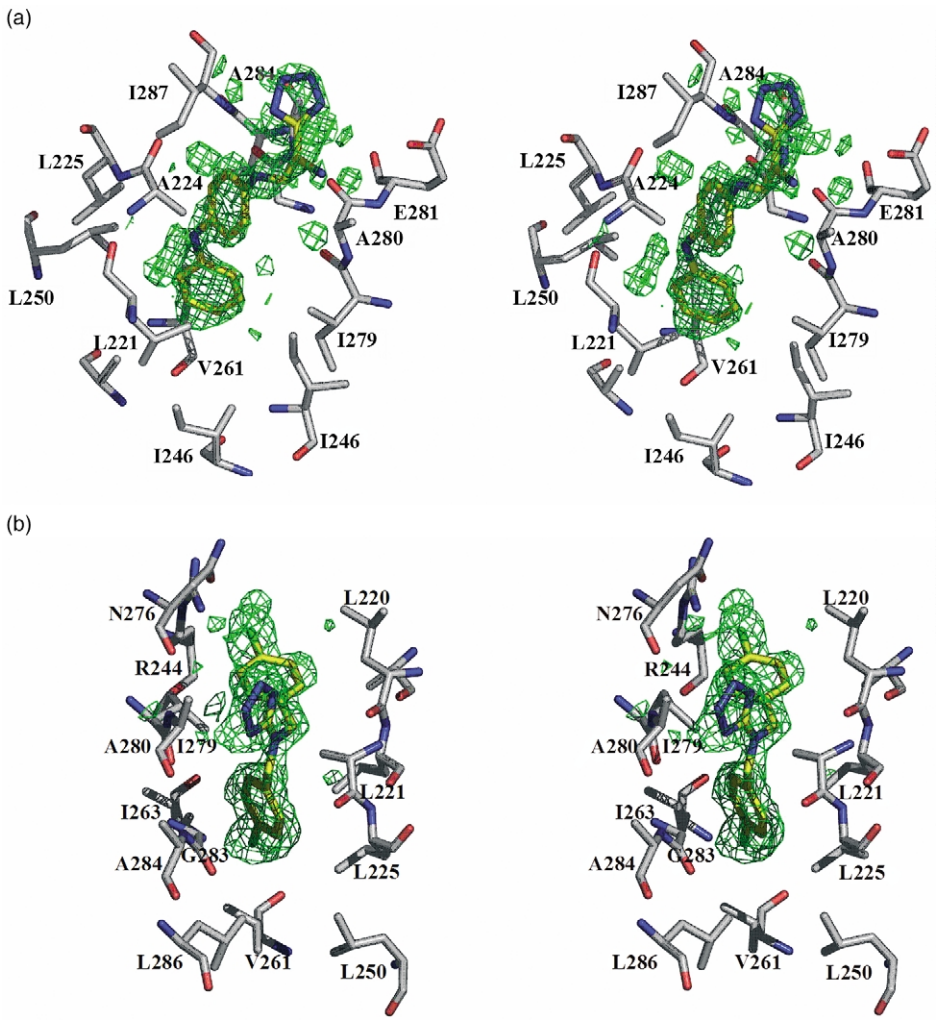

Figure 3. Stereo view of omit electron density difference map ($|F_o| - |F_c|$) showing the inhibitor binding site for compound **1** (a) and compound **2** (b). Carbon atoms are shown in yellow (inhibitor) and gray (TEM-1); oxygen atoms are red; nitrogen atoms are blue; and chlorine atoms are green. The map is contoured at 2.5σ. Electron density Figures were generated using the program PYMOL.[30]

Instead of finding the compounds bound to the active site, both were buried between two helices 16 Å from the active site serine (Ser70), disrupting the core (Figure 4). Intriguingly, compound **2** was observed to have a second binding mode that did, at least partly, occlude the traditional active site (near residues Ser235, Gly245, and Gly236) where it had been originally designed to bind. However, it appears that binding to this second site would only be possible to the "opened-up" structure that results after inhibitor binding to the first, core site. Whereas occupancy was not refined, both compound binding sites appear highly occupied as suggested by strong electron density.

Both compounds **1** and **2** penetrate the TEM-1 core through insertion between helices 11 and 12 (residues 219–226 and 271–289, respectively). This "opening up" of secondary structure (Figure 4) results in major backbone and side-chain rearrangement that exposes mainly hydrophobic surface to the compound (Figure 5). For instance, the α-carbon atoms of residues 218–224 (helix 11) move 3–7 Å and those of residue 274–285 (helix 12) move 1–3 Å from apo structure positions. Regions distant from this cryptic binding site remain unperturbed (Figure 4). rmsd values for α-carbon atoms between the TEM-1 structure (previously determined),[9] and the TEM-1 complexes with compound **1** and **2** are both 0.92 Å. Each compound makes extensive interactions with residues Ile246, Val261 and Ile263, which form the base of the new pocket, and Leu221, Leu250, Ile279, and Leu286 which form the surrounding walls (Figure 5). The solvent accessible surface area of these residues is 14 Å^2 in the apo state (PDB structure 1jwp),[9] 184 Å^2 and 153 Å^2 in the binding competent unbound state (calculated by removing the coordinates of each compound), and 100 Å^2 and 33 Å^2 in the compound-bound state for the structure with compound **1** and **2**, respectively. These values highlight the extensive core surface area that is exposed when moving from the apo state to the binding competent state. The majority of

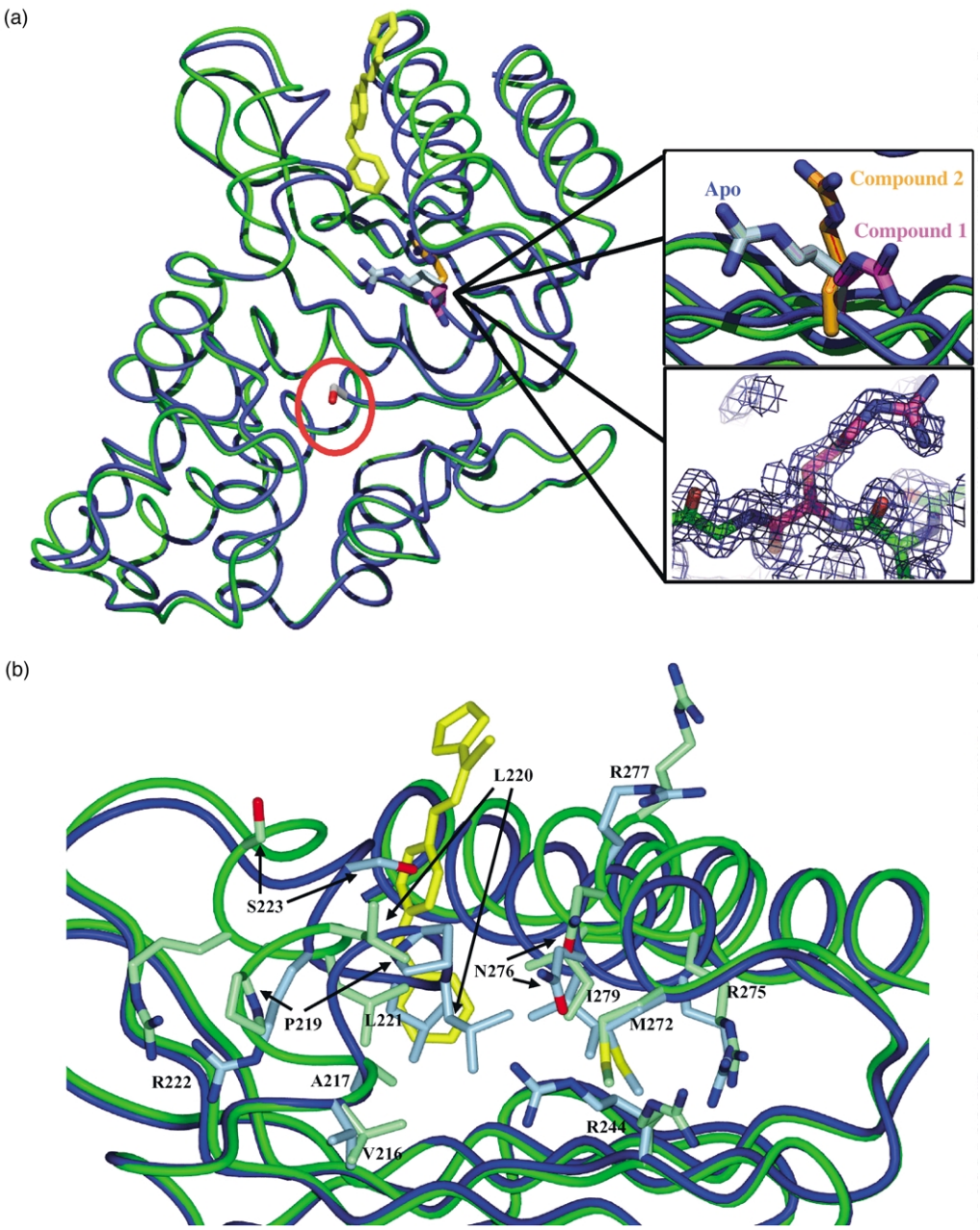

Figure 4. The conformational rearrangement upon inhibitor binding. (a) α-Carbon representation of TEM-1 before and after inhibitor binding. The catalytic serine 70 is circled. Apo-TEM, blue tube; compound **1**-bound TEM, green. Upper inset displays the conformation of Arg244 in the three different crystal structures: apo (blue), compound **1** bound (magenta), and compound **2** bound (orange). Lower inset displays the $2F_o - F_c$ map of Arg244 from the complex of TEM-1 with compound **1**. (b) Structure of TEM residues that change conformation upon binding compound **1** and link the inhibitor binding site with the enzyme's active site. Figure generated using the programs MOLMOL[31,32] and POVRAY (http://www.povray.org).

this "new" surface area is subsequently buried in the complex due to the formation of new protein–compound interactions.

The disruption of core interactions results in large conformational changes in Arg244. This residue is thought to be important for catalytic activity;[10,11] it interacts with the canonical C3′ carboxylates of β-lactam substrates in several crystal structures and its substitution diminishes catalytic activity substantially. Whereas this arginine is normally well packed in TEM structures, in these complexes it is unmoored from its usual interactions and occupies a different non-native conformation in each complex (Figure 4). Correspondingly, the terminal side-chain atoms of Arg244 in both complexes have poorly resolved electron density and relatively high *B*-factors, correlating with higher side-chain motion. The new conformations and motion of this arginine appear to result from the loosening of packing

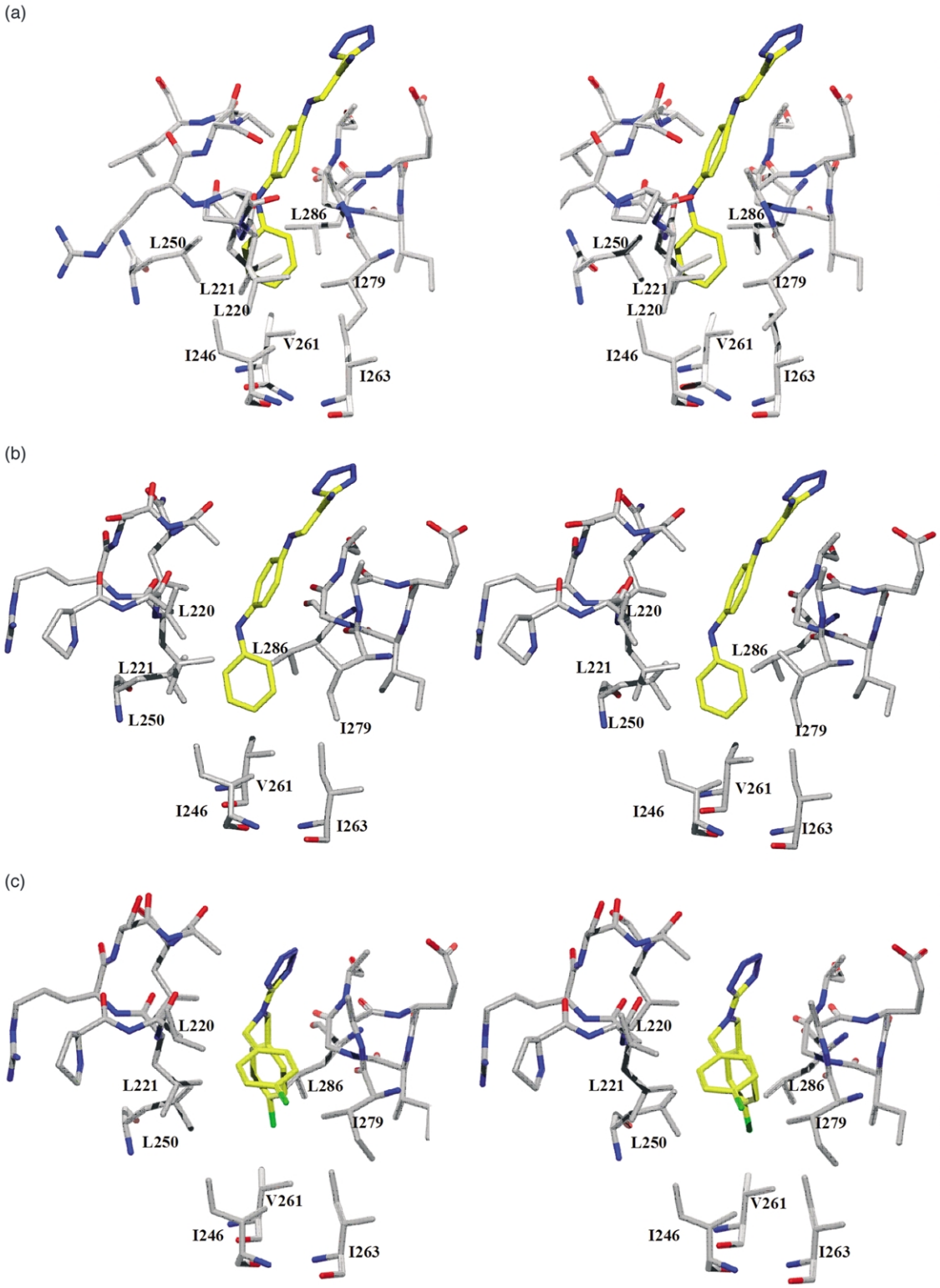

Figure 5. Stereo-view of inhibitor binding sites. (a) Apo state of TEM-1. Compound **1** is overlaid in binding site for orientation purposes. (b) Binding site for compound **1**. (c) Binding site for compound **2**. Gray, TEM-1 carbon atoms; yellow, inhibitor carbon atoms; blue, nitrogen atoms; red, oxygen atoms, green, chlorine atoms.

interactions upon opening up the two helices. Leu220, a residue of helix 11, and Asn276, a residue in helix 12, which previously helped orient Arg244 through a packing interaction (3.7 Å) and hydrogen bond (2.9 Å), respectively,[9] move 6.0 Å (6.4 Å in compound **2** structure) and 5.2 Å (4.8 Å in compound **2** structure) away from Arg244 upon inhibitor binding (Figure 4(b)). Leu220 and Asn276 both become more solvent exposed as a result of an overall unzipping of helices 11 and 12, in particular

occurring at the ends that face near the active site. This concerted movement is likely aided by the conformational constraints of a proline residue (Pro219) within helix 11.

Discussion

The structures of these inhibitor complexes provide a snapshot of what had previously been only a theoretical construct. These inhibitors not only bind to the denatured state of the enzyme, as they do at higher temperatures, but also to a folded form at lower temperatures. This highlights the key role that temperature can have in binding, especially for hydrophobic ligands. Changes in temperature cannot only alter affinity, but can completely change the dominant mode of binding. Therefore, these structures offer a concrete example of a situation recently anticipated as a formal possibility by Waldron & Murphy, who described the pattern of stability change and inhibition that would result from a molecule that could bind to both folded and unfolded forms of a protein (Figure 1).[6] Indeed, the structures define not only recognition by the folded form, but suggest how they might bind the unfolded state, where large hydrophobic patches will be revealed. The structures are also examples of inhibition occurring through something as extreme as disruption of structural packing; binding sites can be revealed even in the highly packed core of a protein. It is appropriate to consider how such cryptic sites might be recognized in other proteins, and to consider their prospects as targets for small molecule inhibitors.

In hindsight, there are several structural features that might have suggested the possibility of opening up a binding site in the region of helixes 11 and 12. One is the unfavorable phi/psi angles (−97.5/−129.6) adopted by Leu220 (within the N-terminal end of helix 11) in previous structures of TEM-1,[9,12] even at 0.85 Å resolution.[13] As a consequence of inhibitor binding and helix opening, Leu220 switches to favorable phi/psi angles (−70.5/−44.8, compound **1**; and −66.5/−43.6, compound **2**), presumably relieving conformational strain and partially counterbalancing the energetic cost of core disruption. Consistent with this view, the COREX algorithm, which has suggested structural linkages between allosteric binding sites and active sites,[14–16] predicts that the region where compounds **1** and **2** bind is relatively unstable.[17] Both of these observations suggest that helixes 11 and 12 of TEM-1, though apparently well-packed, are more predisposed than other core regions to adopt another conformation.

Even more compelling than computational prediction, it turns out that the cryptic site to which compounds **1** and **2** bind has been observed previously. Although at the time we determined them we were unaware of the existence of this cryptic site in class A β-lactamases, we have subsequently learned that an almost identical site was observed in the structure of SHV β-lactamase, which shares 68% sequence identity with TEM-1. In this structure, determined by Knox, Bonomo, and colleagues,[18] a molecule of crystallizing adjuvant, Cymal-6 (cyclohexyl-hexyl-β-D-maltoside), occupies the same cryptic site as compounds **1** and **2**. Similar to these complexes, the Cymal-6 buried its long, hydrophobic tail in the pocket, exposing its sugar head-group to the solvent (see structure, Table 1). Also like the complexes discussed here, the complex with Cymal-6 disrupts the catalytically competent conformation of Arg244 in SHV-1, weakly inhibiting the enzyme. The similarity of the cryptic sites revealed in these three complexes, and the chemical dissimilarity of the inhibitors, suggests that this site is relatively low energy, and that inhibition on the part of these molecules is driven by biophysical properties such as hydrophobic surface area burial. It is, therefore, not surprising that van't Hoff analysis of the inhibition data suggests that the thermodynamics of binding for both inhibitors are dominated by an entopic term that contributes ~98% of the free energy at 25 °C (data not shown), consistent with hydrophobic burial.[19] Such entropically driven binding also suggests a model for the mode of interaction with the unfolded state at higher temperature.

With the structure of this "cryptic" site determined, indeed, determined several times, it becomes a legitimate target for further inhibitor discovery. The packing site occupied by compounds **1** and **2** appears well-suited to binding small molecules, offering a large hydrophobic surface, considerable shape specificity, and several polar groups at the top of the site. Whereas compounds **1** and **2** are relatively weak inhibitors, they bind to TEM-1 with some specificity (Table 1). Inhibition on the part of all three ligands for this site, including Cymal-6, appears to be driven largely by hydrophobic complementarity, it may be possible to design or discover other molecules that can complement this site specifically and bind with improved affinity.

One way to do so would be to find molecules that better complement this cryptic site. For instance, in the complex with compound **1**, 70 Å^2 of surface area, which are buried in the apo-conformation of the enzyme, remain exposed. This surface is a contiguous segment (residues Leu221, Ile246, Ile263, and Ile279), which makes it an attractive target for inhibitor design. It may be possible to design analogs of compound **1** that complement this exposed hydrophobic surface, improving affinity. Whether or not such optimized analogs could make up the core-disruption penalty to achieve "drug-like" affinities is presently unclear.

In summary, the structures of these inhibitor–enzyme complexes not only reduce to atomic resolution a mechanism of inhibition that heretofore may have been considered a curiosity of linked equilibria, but also offer the chance to

discover further inhibitors that, by their nature, will be novel. For many targets, including antibiotic resistance enzymes like β-lactamase, there is much need for such novel inhibitors.

Materials and Methods

Enzymology

TEM-1 ($\epsilon_{281} = 29{,}400\ cm^{-1}\ M^{-1}$) and TEM mutants M182T and G238A were expressed in a protease-deficient *Escherichia coli* SF120 strain and purified by a standard procedure described elsewhere.[9,20,21] 3-(4-Phenylamino-phenylamino)-2-(1H-tetrazol-5-yl)-acrylonitrile (compound **1**) and *N*,*N*-bis(4-chlorobenzyl)-1H-1,2,3,4-tetraazol-5-amine (compound **2**) were Maybridge Chemicals compounds obtained from Ryan Scientific (Isle of Palms, SC, USA). For each compound, 50 mM stock solutions were prepared in dimethyl sulfoxide (DMSO). All enzyme assays were performed in 50 mM Tris (pH 7.0) with and without the presence of 0.1 mg/ml saponin or 0.1% Triton-X100. DMSO concentration was always kept below 5%. Furyl-acrylpenicillanic acid (FAP, Calbiochem, La Jolla, CA) and nitrocefin (Oxiod, Basingstoke, Hampshire, England) were used as TEM-1 substrates. Trypsin and MDH assays conditions were followed as described.[8,22] β-Trypsin (bovine pancreatic), malate dehydrogenase, *N*-benzolyl-L-arginine ethyl ester (BAEE), oxaloacetate, and reduced β-nicotinamide adenine dinucleotide (NADH) were purchased from Sigma (St. Louis, MO). Enzyme reactions were monitored at 340 nm (FAP and NADH), 482 nm (nitrocefin), and 260 nm (BAEE). Kinetic parameters k_{cat}, K_m, and K_i were determined by initial velocity non-linear regression analysis using KalidaGraph (Synergy Software, Reading, PA).

Thermal denaturation

TEM-1 was denatured by raising the temperature in 0.1 deg. C increments (ramp rate of 2 deg. C/minute) in 50 mM phosphate buffer (pH 7.0), using a Jasco 715 spectrapolarimeter with a Peltier-effect temperature controller and an in-cell temperature monitor. The unfolding transition of TEM-1 in the presence of compound **2** was monitored by the integrated emission fluorescence above 300 nm (using a cut-off filter) from excitation at 295 nm, whereas compound **1** was monitored by the far-UV CD (223 nm) signal due to a high intrinsic fluorescence. A least-squares regression fit using a two-state model was performed using the program Exam[21,23] to determine the t_m and van't Hoff $\Delta H°$ of unfolding. The change in heat capacity upon denaturation (ΔC_p) was set to 3.8 kcal/mol K (16.0 kJ/mol K) for each enzyme and complex.

Crystal growth and structure determination

Crystals of TEM were grown as described.[9,24] Compounds were introduced by soaking TEM crystals in a solution of 1.4 M potassium phosphate (pH 8.3) containing 1.25 mM compound. TEM-1 wild-type crystals were soaked with compound **1** for 12 hours and crystals of TEM-1 M182T were soaked with compound **2** for one hour. DMSO, which is used to dissolve both compounds, was kept to below 2.5% in final buffer conditions.

Crystals were submerged in a cryo-protectant solution of 25% (w/v) sucrose, 1.25 mM compound, and 1.6 M potassium phosphate (pH 8.3) for approximately 30 seconds, mounted on nylon loops and then flash frozen in liquid nitrogen. The diffraction data were collected using single crystals at the Advanced Photon Source (Argonne, IL) on beamline 5-ID ($\lambda = 0.97014$ Å; 100 K) using a MARCCD detector. Data were processed with the MOSFLM/SCALEPACK package[25] to 1.45 Å (compound **1**) and 1.90 Å (compound **2**). The apo-structure of the WT* TEM mutant M182T, which has been determined to 0.85 Å resolution[13] was used as an initial model for molecular replacement. Unambiguous electron density for the inhibitors and the movement of the protein was present in the initial $F_o - F_c$ electron density maps. The structures were initially refined by rigid-body refinement, followed by cycles of Cartesian and *B*-factor refinement using the CCP4 suite[26] of programs. Map fitting for inhibitors and for moved protein regions was done in O[27] and Turbo.[28] Electron density maps identified a second binding site located between TEM-1 packing contacts. This position is attributed to crystal contacts and is not expected to be a binding site in solution. Accessible surface area calculations were performed using the program NACCESS.[29]

Protein Data Bank accession codes

The structures of the TEM-1 complexes with compounds **1** and **2** have been deposited with the RCSB PDB with accession codes 1PZO and 1PZP.

Acknowledgements

This work was supported by NIH grant GM59957 (to B.K.S.) and by training grant number 1T32AG000260-01 through the Drug Discovery Program of Northwestern University (to J.R.H., L. Van Eldik PI). We thank G. Minasov for help in obtaining suitable crystals and aid in crystallographic processing and Pamela Focia for synchrotron help. We also thank John Irwin, Beth Beadle, Yu Chen, & Susan McGovern for reading the manuscript. X-ray data were collected at the DND-CAT at the Advanced Photon Source (APS). DND-CAT is supported by the DuPont Co., the Dow Chemical Co., National Science Foundation, and the State of Illinois. Use of the APS is supported by the US Department of Energy under contract W-31-102-Eng-38.

References

1. Miller, D. W. & Dill, K. A. (1997). Ligand binding to proteins: the binding landscape model. *Protein Sci.* **6**, 2166–2179.
2. Arkin, M. R., Randal, M., DeLano, W. L., Hyde, J., Luong, T. N., Oslob, J. D. *et al.* (2003). Binding of small molecules to an adaptive protein–protein interface. *Proc. Natl Acad. Sci. USA*, **100**, 1603–1608.
3. Braisted, A. C., Oslob, J. D., Delano, W. L., Hyde, J., McDowell, R. S., Waal, N. *et al.* (2003). Discovery of a potent small molecule IL-2 inhibitor through fragment assembly. *J. Am. Chem. Soc.* **125**, 3714–3715.

4. Esnouf, R., Ren, J., Ross, C., Jones, Y., Stammers, D. & Stuart, D. (1995). Mechanism of inhibition of HIV-1 reverse transcriptase by non-nucleoside inhibitors. *Nature Struct. Biol.* **2**, 303–308.
5. Ren, J., Nichols, C., Bird, L., Chamberlain, P., Weaver, K., Short, S. *et al.* (2001). Structural mechanisms of drug resistance for mutations at codons 181 and 188 in HIV-1 reverse transcriptase and the improved resilience of second generation non-nucleoside inhibitors. *J. Mol. Biol.* **312**, 795–805.
6. Waldron, T. T. & Murphy, K. P. (2003). Stabilization of proteins by ligand binding: application to drug screening and determination of unfolding energetics. *Biochemistry*, **42**, 5058–5064.
7. McGovern, S. L., Caselli, E., Grigorieff, N. & Shoichet, B. K. (2002). A common mechanism underlying promiscuous inhibitors from virtual and high-throughput screening. *J. Med. Chem.* **45**, 1712–1722.
8. McGovern, S. L. & Shoichet, B. K. (2003). Kinase inhibitors: not just for kinases anymore. *J. Med. Chem.* **46**, 1478–1483.
9. Wang, X., Minasov, G. & Shoichet, B. K. (2002). Evolution of an antibiotic resistance enzyme constrained by stability and activity trade-offs. *J. Mol. Biol.* **320**, 85–95.
10. Moews, P. C., Knox, J. R., Dideberg, O., Charlier, P. & Frere, J. M. (1990). Beta-lactamase of *Bacillus licheniformis* 749/C at 2 Å resolution. *Proteins: Struct. Funct. Genet.* **7**, 156–171.
11. Zafaralla, G., Manavathu, E. K., Lerner, S. A. & Mobashery, S. (1992). Elucidation of the role of arginine-244 in the turnover processes of class A beta-lactamases. *Biochemistry*, **31**, 3847–3852.
12. Wang, X., Minasov, G. & Shoichet, B. K. (2002). The structural bases of antibiotic resistance in the clinically-derived mutant beta-lactamases TEM-30, TEM-32, and TEM-34. *J. Biol. Chem.* **10**, 10.
13. Minasov, G., Wang, X. & Shoichet, B. K. (2002). An ultrahigh resolution structure of TEM-1 beta-lactamase suggests a role for Glu166 as the general base in acylation. *J. Am. Chem. Soc.* **124**, 5333–5340.
14. Hilser, V. J. & Freire, E. (1996). Structure-based calculation of the equilibrium folding pathway of proteins. Correlation with hydrogen exchange protection factors. *J. Mol. Biol.* **262**, 756–772.
15. Hilser, V. J., Dowdy, D., Oas, T. G. & Freire, E. (1998). The structural distribution of cooperative interactions in proteins: analysis of the native state ensemble. *Proc. Natl Acad. Sci. USA*, **95**, 9903–9908.
16. Pan, H., Lee, J. C. & Hilser, V. J. (2000). Binding sites in *Escherichia coli* dihydrofolate reductase communicate by modulating the conformational ensemble. *Proc. Natl Acad. Sci. USA*, **97**, 12020–12025.
17. Luque, I. & Freire, E. (2000). Structural stability of binding sites: consequences for binding affinity and allosteric effects. *Proteins: Struct. Funct. Genet.* (Suppl.), **63–71.**
18. Kuzin, A. P., Nukaga, M., Nukaga, Y., Hujer, A. M., Bonomo, R. A. & Knox, J. R. (1999). Structure of the SHV-1 beta-lactamase. *Biochemistry*, **38**, 5720–5727.
19. Ross, P. D. & Subramanian, S. (1981). Thermodynamics of protein association reactions: forces contributing to stability. *Biochemistry*, **20**, 3096–3102.
20. Dubus, A., Wilkin, J. M., Raquet, X., Normark, S. & Frere, J. M. (1994). Catalytic mechanism of active-site serine beta-lactamases: role of the conserved hydroxy group of the Lys-Thr(Ser)-Gly triad. *Biochem. J.* **301**, 485–494.
21. Wang, X., Minasov, G. & Shoichet, B. K. (2002). Noncovalent interaction energies in covalent complexes: TEM-1 beta-lactamase and beta-lactams. *Proteins: Struct. Funct. Genet.* **47**, 86–96.
22. Powers, R. A., Morandi, F. & Shoichet, B. K. (2002). Structure-based discovery of a novel. Noncovalent inhibitor of AmpC beta-lactamase. *Structure (Camb.)*, **10**, 1013–1023.
23. Kirchoff, W. (1993). EXAM: a two-state thermodynamic analysis program, NIST publication 1401, Gaithersburg Maryland.
24. Strynadka, N. C., Adachi, H., Jensen, S. E., Johns, K., Sielecki, A., Betzel, C. *et al.* (1992). Molecular structure of the acyl-enzyme intermediate in beta-lactam hydrolysis at 1.7 Å resolution. *Nature*, **359**, 700–705.
25. Leslie, A. G. W. (1992). Recent changes to the MOSFLM package for processing film and image plate data. *Joint CCP4 + ESF-EAMCB Newsletter Protein Crystallog.* No. 26.
26. Collaborative Computational Project No. 5 (1994). The CCP4 suite: programs for protein crystallography. *Acta Crystallog. sect. D*, **50**, 760–763.
27. Jones, T. A., Zou, J. Y., Cowan, S. W. & Kjeldgaard, H. (1991). Improved methods for building protein models in electron density maps and the location of errors in these models. *Acta Crystallog. sect. A*, **47**, 110–119.
28. Cambillau, C. & Roussel, A. (1997). *Turbo Frodo, OpenGL* edit., Universite Aix-Marseille II, Marseille, France.
29. Hubbard, S. J. & Thornton, J. M. (1993). *NACCESS, Computer Program V2.1.1*, edit, Department of Biochemistry and Molecular Biology, University College London.
30. DeLano, W. L. (2002). *The PyMOL Molecular Graphics System*, DeLano Scientific, San Carlos, CA.
31. Koradi, R., Billeter, M. & Wuthrich, K. (1996). MOLMOL: a program for display and analysis of macromolecular structures. *J. Mol. Graph.* **14**, 51–55.
32. Koradi, R., Billeter, M. & Wuthrich, K. (1996). MOLMOL: a program for display and analysis of macromolecular structures. *J. Mol. Graph.* **14**, 29–32.

Edited by I. Wilson

(Received 29 August 2003; received in revised form 9 December 2003; accepted 23 December 2003)